Energy Syst (2018) 9:1095–1113
https://doi.org/10.1007/s12667-017-0250-z

ORIGINAL PAPER

Worst-case temporal aggregate power ramp distributions for a PAC wind turbine

Sanjoy Roy[1]

Received: 11 November 2016 / Accepted: 2 September 2017 / Published online: 15 September 2017

Abstract As a critical component for evaluation of output power variability at wind farms, short duration power ramp distributions are typically evaluated as ensemble estimates across elaborate time-aggregated compilation of on-site field measurements. This paper proposes an algorithmic alternative to the above, by introducing statistical estimates both for probability density function (pdf) and cumulative distribution function (cdf) of power ramps. The estimates are pessimistic as possible real time filtering, attributable to turbine inertia and time-constants, is assumed to be negligible. The proposed algorithm is conveniently implemented on popular spreadsheet software, has limited dependence on source wind statistics, and easily accommodates turbulence conditions given by the IEC 61400-1 standards. Its application is illustrated for the popular Vestas V-90 3 MW turbine, assumed to operate at a site with source wind accordingly specified.

Keywords Wind energy · Wind power generation · Power ramp distributions · Statistical estimates

For formulations that involve time-varying short duration variability within a long time horizon, "N" is assumed to represent the total possible *number of distinct variability conditions* that may occur. For summation or aggregation purposes, these are indexed as $i = 1, 2, \ldots, N$. It may be noted that at any time, the source wind may face only one of the N variability conditions. Whenever variables and parameters (listed below) refer to the i-th variability conditions, they are provided appropriate subscripts in the text.

Electronic supplementary material The online version of this article (doi:10.1007/s12667-017-0250-z) contains supplementary material, which is available to authorized users.

✉ Sanjoy Roy
roys@iitrpr.ac.in

1 Department of Electrical Engineering, Indian Institute of Technology, Rupnagar, Punjab 140 001, India

Nomenclature

Short duration variables, statistical functions, and associated parameters:

C :	*Scale parameter* for Weibull distribution of wind speed.
f :	Long duration *temporal fraction of occurrence* for a specific short duration source wind condition; that is, the fraction of a long time horizon (say, days or months) across which a particular variability condition may occur.
$P(.)$:	Output power of wind turbine (as a function of source wind speed).
u :	Source wind speed.
$\bar{u}$:	*Short duration mean* value of source wind speed (constant for a short time horizon, but may vary over longer duration).
$\hat{u}$:	Short duration *maximum likelihood* value of source wind speed ("most probable" or modal value; constant for a short time horizon, but may vary over longer duration).
Δu :	Random change in the source wind speed from its *maximum likelihood* value in short duration (that is, in short duration, $\Delta u = u - \hat{u}$).
$\Gamma(.)$:	The complete gamma function.
κ :	*Shape parameter* for Weibull distribution of wind speed.
$\Delta\mu$:	Output power ramp (that is, change in $P(.)$), normalised by P_{rat}.
ρ :	Rayleigh distribution modal parameter for long duration wind speed.
σ :	*Short duration standard deviation* of source wind speed (constant for a short time horizon).
τ_{15} :	*Turbulence intensity* at 15m sensor height as defined by IEC 61400-1 standards.
$\phi(.)$:	Probability density function for normalised power ramps, given short duration source wind conditions.
$\langle\phi(.)\rangle$:	Probability density function (pdf) for normalised power ramp, aggregated over a range of short duration source wind conditions.
$\varphi(.)$:	Long duration probability density function for source wind speed.
$\Phi(.)$:	Cumulative distribution function (cdf) for speed or power ramps, for given short duration source wind conditions.

PAC turbine specifications obtained, or derived from manufacturer's data-sheets:

a, b, m :	Parameters to fit the *Weibull sigmoid* function to a specific $\mu(.)$ function.
P_{rat} :	Rated value of power output by the turbine unit.
u_{in} :	*Cut-in* value of source wind speed.
u_{rat} :	Rated value of source wind speed.
u_{out} :	*Cut-out* value of source wind speed.
$\mu(.)$:	Output power normalised by P_{rat} of the turbine unit under steady, streamlined source wind.

1 Introduction

With growth of wind based power generation, *short duration power variations* at the output of active pitch angle controlled (PAC) turbines has been recognised as inevitable fallout of turbulence and gusts in the source wind [1,5]. Following from the common inference that wind variations within time horizon of minutes or less are best represented as stochastic changes rather than deterministic ones [6], short duration power variations have been analysed using probability density functions (pdf's) and cumulative distribution functions (cdf's) of generated power; both functions being fundamental to analysis of random numbers and signals (for example, [7]). By contrast, *medium* and *long duration* variations that stretch from several minutes to hours [2,3] may be appropriately represented as deterministic changes. A comprehensive briefing on source wind variations, inclusive of categorisation by duration, is provided in [6].

While speed or power ramps within source wind are of importance to the turbine in several engineering contexts (structural loading and stress [8], and real time control [9] being selected examples); short duration power variations at the output of a PAC turbine (or a turbine cluster) are critical to integrated network performance and management [3–5,9,10]. Alternatively referred to as "power ramp distributions", pdf's and cdf's of the power variations are useful in at least four ways:

i. *Evaluation of dispatchability* [11], which covers the following expectations:
   - Availability of wind based generation precisely on-demand,
   - Supply availability independent of proximity between load centres and wind turbines,
   - Preferred temporal coherence between wind based generation and load variations, and
   - Possible performance parity between wind based and conventional generators in real time.

ii. *Spatial aggregation* to smoothen power variations in time [12,13]: a common approach in cases where wind based generators are spread across significant area.

iii. *Decisions regarding storage requirement* [9,14,15], which are always important with reference to storage technology and associated capital overheads.

iv. *Reserve regulation and planning*, which involves conventional sources within the system to which wind turbines are integrated [16–18].

Despite their usefulness, pdf's and cdf's of short duration output power ramps have themselves not been very easy to compile; precise field measurements (empirical approach), or elaborate aerodynamic simulations or mesoscale models (simulation approach) being the two popular methods. By either approach, the analyst is faced with substantial volume of sampled data, which is to be subsequently sorted according to frequency of occurrence. The resulting compilations, which are rather computationally intensive as well as susceptible to measurement and data logging errors, will be referred to as "ensemble estimates" in the discussions to follow.

A largely algorithmic and easily programmable alternative to the ensemble estimate is introduced in this paper. Since the approach depends on prior knowledge of short duration mean wind speed and the associated standard deviation, the nomenclature "statistical estimate" seems appropriate for the resulting distributions. Other than the obviously modest computational requirement, certain objective advantages associated with statistical estimates add to their usefulness:

a. By suitable spreadsheet software, statistical estimates can be computed at planning stage for any proposed wind turbine installation site [6,15].
b. It follows from "a" that dependent decisions on
   - choice of commercially available turbine makes,
   - spatial distribution of turbines,
   - storage support, and
   - reserve regulation,

   all of which may influence capital investment as well as network performance, can be convenient and quick [9–18].
c. Applicability of statistical estimates to typical PAC characteristics is easy. Specification of such characteristics can assume the minimal numeric form of wind-speed/output-power pairs (or alternative graphical forms) that is commonly available from turbine manufacturers [19,20].
d. For a turbine cluster spread across a wind farm, "c" can be extended to an *aggregate output power curve* [21,22].
e. Statistics of source wind in the minimal numeric form of mean-wind-speed/standard-deviation pairs [6] are the only prerequisites for statistical estimates.
f. As proposed, statistical estimates can conveniently use short duration wind speed and standard deviation data provided in IEC 61400-1 standards, or comparable alternatives [23,24].

The computation algorithm is based on certain core assumptions, some of which make statistical estimates pessimistic, or "worst-case" estimates. The assumptions are summarised below, and subsequently revisited as and where relevant:

A1. Within horizons of short duration (minutes or less), the source wind speed is random, and follows the well established two-parameter Weibull distribution [6, 7].

A2. Corresponding to any short duration mean wind speed, the *maximum likelihood wind speed* is the most commonly occurrent in time, as directly implied by its definition.

A3. While operating at a particular mean wind speed, short duration changes occur predominantly from the corresponding maximum likelihood value to higher or lower speeds. This assumption essentially follows from A2. It should be noted however that relatively infrequent "direct changes" from speeds greater than the maximum likelihood to those less than the same (or vice versa) are not ignored. Rather, such variations are taken into consideration as two successive changes (from a higher speed to the maximum likelihood, followed by a second change from the maximum likelihood to a lower speed, or vice versa).

A4. Filtering action of PAC dynamics on short duration wind variations is negligible. This essentially implies very fast responsive turbine and controller, so that short duration wind variations are "converted" to power changes according to the turbine power curve (as in advantage "c") or the aggregate turbine-cluster power curve (as in advantage "d" above).

A4 is perhaps the strongest of the four assumptions, because turbine inertia and PAC time constants always filter the dynamics of any practical configuration. Precise conclusions are difficult to draw because of the variety of PAC turbine configurations that are commercially available. However the statement of A4 is easy to appreciate as one of pessimistic, worst-case dynamics.

Analytical concepts on short duration power ramp distributions are formulated in Sect. 2; and culminate in a set of algorithmic steps for computation of statistical estimates. Section 3 describes background to an example case, for which detailed power ramp distributions and their temporal aggregates are presented in Sect. 4. Evolving the example further, Sect. 5 presents sensitivity of temporal aggregate power ramp distributions to the most probable value of short duration mean wind speed.

2 Conceptual formulations for statistical estimates

2.1 Probability distribution for short duration speed ramps

If wind speed u at a specific turbine hub-height is assumed to follow a two-parameter Weibull pdf (as A1 above) given by

$$p\left(u\right)=\frac{\kappa}{C}\left(\frac{u}{C}\right)^{\kappa-1}.\exp\left[-\left(\frac{u}{C}\right)^{\kappa}\right] \tag{1}$$

with C and κ as *short duration scale* and*shape factors* respectively [7], then the short duration mean wind speed $\bar{u}$ follows as

$$\bar{u}=C.\Gamma\left(1+1/\kappa\right) \tag{2}$$

As noted in point "e" of Sect. 1, the formulations to follow require the short duration mean wind speed $\bar{u}$ and standard deviation σ. Ratio of the two is defined as the *turbulence intensity* "τ" ($\tau \triangleq \sigma/\bar{u}$), and is a useful parametric measure of short duration wind variations [6]. For example, within the loose range of $1 \lesssim k \lesssim 10$, the shape parameter is given by [25]

$$\kappa \approx \left(\sigma/\bar{u}\right)^{-1.086} \tag{3}$$

For a known value of τ therefore, (3) provides a convenient way to calculate κ; following which C can be obtained by (2).

Equating the derivative of (1) to zero, followed by some simplification, leads to the most probable wind speed for the given values of $(\bar{u}, \sigma)$ (hence C and κ). This value can be termed as the maximum likelihood wind speed (refer assumption A3, Sect. 1), and is obtained as [7]:

$$\hat{u}=C.\left(1-1/\kappa\right)^{1/\kappa} \tag{4}$$

By assumption A3, majority of speed ramps are expected to occur as changes around $\hat{u}$; with the latter as the most common value in time. For all short duration speed changes from $\hat{u}$ to values "within" some $\hat{u} + \Delta u$ (Δu may be of either sign), the cdf is obtained as

$$\begin{aligned}
&\Phi\left(\hat{u} \rightarrow u | u \in \left[\hat{u}, \hat{u} + \Delta u\right], C, \kappa\right) \\
&= \int_{\hat{u}}^{\hat{u}+\Delta u} p\left(u\right).du = \exp\left[-\left(\frac{\hat{u}}{C}\right)^{\kappa}\right] - \exp\left[-\left(\frac{\hat{u}+\Delta u}{C}\right)^{\kappa}\right] \\
&= \exp\left[\frac{1-\kappa}{\kappa}\right] - \exp\left[-\left(\frac{\hat{u}+\Delta u}{C}\right)^{\kappa}\right]
\end{aligned} \tag{5}$$

while the pdf is a derivative of (5) with respect to Δu

$$\frac{\partial}{\partial \Delta u}\Phi\left(\hat{u} \rightarrow u | u \in \left[\hat{u}, \hat{u} + \Delta u\right], C, \kappa\right) \frac{\kappa}{C}\left(\frac{\hat{u}+\Delta u}{C}\right)^{\kappa-1}.\exp\left[-\left(\frac{\hat{u}+\Delta u}{C}\right)^{\kappa}\right] \tag{6}$$

2.2 Generic function for PAC output power curve

The advantage listed as "c" in Sect. 1, states a minimal specification of the PAC characteristic in terms of output-power for different admissible values of wind-speed [19,20]. PAC output power curves can be thus described as

$$P\left(u\right) = \mu\left(u\right).P_{rat} \tag{7}$$

where P_{rat} is the rated power of the specific turbine, and $\mu\left(u\right)$ is the *ideal zero-turbulence output coefficient*—the fraction of rated power that the turbine outputs with steady streamlined wind speed u. For most PAC turbines, $\mu\left(u\right)$ has a generic form

$$\mu(u) = \begin{cases} 0; & if\ u \le u_{in} \\ \text{an increasing fraction } 0 \longrightarrow 1; & if\ u_{in} \le u \le u_{rat} \\ 1; & if\ u_{rat} \le u \le u_{out} \\ 0; & if\ u > u_{out} \end{cases} \tag{8}$$

with u_{in}, u_{rat}, and u_{out} as cut-in, rated, and cut-out wind speeds at the hub, respectively [6].

On most well supported spreadsheet platforms, some effort is required to programme (8) in terms of piecewise linear functions using wind-speed/output-power specifications as mentioned above. However, $\mu\left(u\right)$ is considerably more convenient to work with if represented by a continuous differentiable function over the entire range of speed up to *cut-out*. Since the first three segments of (8) describe an "asymmetric sigmoid" [26], replacement by a *Weibull sigmoid* [27] is a good option:

$$\mu(u) = \left\{\begin{array}{ll} 1 - exp[-(a.u - b)^{m}]; & if\ 0 < u \le u_{out} \\ 0; & if\ u > u_{out} \end{array}\right\} \tag{9}$$

Shape of the Weibull sigmoid in (9) is decided by parameters a, b, and m; all of which are to be determined from the wind-speed/output-power data-pairs specified by the turbine manufacturer. This can be easily done by converting the sigmoid to its equivalent logarithmic form:

$$\ln[a] + \ln[u - b/a] = (1/m) . \ln[-\ln[1 - \mu(u)]] \tag{10}$$

The steps to determine a, b, and m, follow from (10):

- from the output power curve specification of the turbine, power data $P(u)$ are normalised by rated power P_{rat}, converting them to ideal zero-turbulence output coefficients $\mu(u)$ in per-unit.
- similarly, the speed data u are normalised by u_{rat} for conversion to per unit.
- A linear curve fit function (available as part of most spreadsheet or graphing software) may be used to obtain an approximate linear function between $\ln[u - b/a]$ and $\ln[-\ln[1 - \mu(u)]]$. This exercise may commence with b/a set to zero, which can be progressively modified to obtain a good linear fit of desired accuracy [28].
- once an acceptable linear approximation is obtained, b/a is known from the set value, while a and m can be calculated from the slope and intercept of (10). This would complete estimation of (9) from the ideal zero-turbulence output power curve as specified numerically or graphically by the manufacturer.

2.3 Statistical estimate of power ramp pdf's and cdf's at different average source wind speed

In Sect. 2.1 (for given values of $\bar{u}$, σ, and hence $\hat{u}$, by (3), (2), and (4)), short duration speed ramps were assumed from $\hat{u}$ to u within the closed range $u \in \left[\hat{u}, \hat{u} + \Delta u\right]$. With all parameters of (9) known, the possible limit of wind speed change Δu corresponds to a per-unit short duration power ramp limit $\Delta\mu$ such that

$$\begin{aligned} \Delta\mu &= \exp\left[-\left(a.\hat{u} - b\right)^m\right] - \exp\left[-\left(a.\left\{\hat{u} + \Delta u\right\} - b\right)^m\right] \\ \Longrightarrow \hat{u} + \Delta u &= \frac{\sqrt[m]{-\ln\left[\exp\left[-\left(a.\hat{u} - b\right)^m\right] - \Delta\mu\right]} + b}{a} \end{aligned} \tag{11}$$

For a specific value of $\bar{u}$, the pdf for signed short duration power ramps is easily obtained in two stages. First, estimates of $\hat{u} + \Delta u$ may be obtained for different values of $\Delta\mu$ by (11), which are power ramps as signed fractions of P_{rat}. Next, the cumulative probability for all ramps not greater than $\Delta\mu$ can be obtained by (5) corresponding to $\hat{u} + \Delta u$.

Though convenient, it should be appreciated that a pdf computed as above is of limited use, since the short duration mean wind speed at any turbine installation is rarely constant across significant lengths of time. A more meaningful temporal aggregate pdf requires two additional steps:

1. The short duration power ramp pdf $\phi_i(\Delta\mu|\bar{u}_i)$ may be obtained corresponding to each (say, i-th) value of short duration mean wind speed.

2. The pdf's thus obtained are to be aggregated over long duration, by weighting them by the *relative frequency of occurrence* for each $\bar{u}_i$ considered for step "1" above.

In order to organise an algorithm to realise the above, pdf's of short duration power ramps are required at the outset.

From the first expression in (11), a differential coefficient of the normalised power ramp with respect to the normalised wind speed ramp is easily obtained as

$$\frac{\partial \Delta\mu}{\partial \Delta u} = ma.\left(a.\left\{\hat{u} + \Delta u\right\} - b\right)^{m-1}.\exp\left[-\left(a.\left\{\hat{u} + \Delta u\right\} - b\right)^{m}\right] \tag{12}$$

Dividing (6) by (12), the statistical estimate of pdf for normalised short duration power ramps is found to be

$$\begin{aligned}
\phi_i\left(\Delta\mu|\bar{u}_i\right) &\triangleq \frac{\partial}{\partial \Delta\mu}\Phi\left(\hat{u}_i \to u|u \in \left[\hat{u}_i, \hat{u}_i + \Delta u\right], C_i, \kappa_i\right) \\
&= \left[\frac{\partial}{\partial \Delta u}\Phi\left(\hat{u}_i \to u|u \in \left[\hat{u}_i, \hat{u}_i + \Delta u\right], C_i, \kappa_i\right)\right].\left[\frac{\partial \Delta\mu}{\partial \Delta u}\right]^{-1} \\
&= \frac{\kappa_i}{ma.C_i}\left(\frac{\hat{u}_i + \Delta u}{C_i}\right)^{\kappa_i - 1}.\left(a.\left\{\hat{u}_i + \Delta u\right\} - b\right)^{1-m} \\
&\quad \times \exp\left[-\left(a.\left\{\hat{u}_i + \Delta u\right\} - b\right)^{m} - \left(\frac{\hat{u}_i + \Delta u}{C_i}\right)^{\kappa_i}\right]
\end{aligned} \tag{13}$$

In (13), κ_i, C_i, and $\hat{u}_i$, are obtained from the i-th short duration mean wind speed $\bar{u}_i$ and standard deviation σ_i by (3), (2) and (4). The limiting short duration ramped speed $\hat{u}_i + \Delta u$ corresponds to each value of per-unit short duration power ramp limit $\Delta\mu$, and can be obtained by (11).

2.4 Weights for short duration mean wind speed: the complete algorithm

Prior to consolidation of steps for statistical estimate of a pdf for short duration power ramps, a procedure for aggregation (refer Sect. 2.3, step "2") across all possible $(\bar{u}_i, \sigma_i)$ needs to be defined.

If across a complete long duration horizon (for example, weeks, months, or season), N+1 different values of short duration mean speed and standard deviation occur as $(\bar{u}_i, \sigma_i)$ pairs for $i = 0, 1, 2, \ldots, N$; then the i-th such wind condition must span across a fraction f_i of the total time horizon, such that

$$\sum_{i=0}^{N} f_i = 1 \tag{14}$$

It must be emphasised that only one out of the $N + 1$ short duration variability conditions may occur at a particular point of time. Further, occurrence of i-th short duration pair $(\bar{u}_i, \sigma_i)$ may prevail across a length of time within the chosen long duration horizon, may change deterministically (precisely known time variation), or may be random. The fraction f_i is therefore not a conventional probability value, and is more appropriately referred to as the i-th *temporal fraction of occurrence*.

With knowledge of the temporal fractions, it is a simple calculation to the temporal aggregate short duration pdf of power ramps:

$$\langle \phi\,(\Delta\mu) \rangle \triangleq \sum_{i=0}^{N} f_i . \phi_i\,(\Delta\mu | \bar{u}_i) \tag{15}$$

An algorithm for statistical estimate of the temporal aggregate short duration power ramp pdf $\langle \phi\,(\Delta\mu) \rangle$ may now be drawn up as follows:

- #1 Across the entire long duration horizon of interest with N+1 different short duration wind conditions ($i = 0, 1, 2, \ldots, N$), the different temporal fractions f_i, and paired values$(\bar{u}_i, \sigma_i)$ of short duration mean wind speed and standard deviation may be noted.
- #2 The short duration Weibull parameters $\kappa_i$and C_i may be obtained using (3) and (2) for each i.
- #3 The short duration maximum likelihood wind speeds may be computed by (4) for each i.
- #4 For the i-th wind condition, with a, b, m, and u_{out} known for the given wind turbine, (11) can be used to compute limiting short duration ramped speeds $\hat{u}_i + \Delta u$ corresponding to different limits of signed short duration power ramps$\Delta\mu$.
- #5 Hence corresponding to each (i-th) wind condition, the pdf $\phi_i\,(\Delta\mu | \bar{u}_i)$ for short duration power ramps$\Delta\mu$ can be obtained by (13).
- #6 #4-5 may be repeated for each short duration wind condition: $i = 0, 1, 2, \ldots, N$. This would result in N+1 pdf's$\phi_i\,(\Delta\mu | \bar{u}_i)$ for short duration power ramps.
- #7 The temporal aggregate short duration power ramp pdf $langle\phi\,(\Delta\mu)\rangle$ may be computed by (15), as a sum of pdf's $\phi_i\,(\Delta\mu | \bar{u}_i)$ weighted by temporal fractions of occurrence f_i.

Steps #8–9 to follow, essentially extend the algorithm #1-7 further so as to compute statistical estimate of the cumulative distribution function for unsigned short duration power ramps. As may be expected, this should involve integration of $[\langle \phi\,(\Delta\mu) + \phi\,(-\Delta\mu) \rangle]$ with respect to differential of the ramp magnitude (pdf's for both positive and negative ramps are summed so as to obtain the pdf for unsigned ramps).

The numerical integration is challenged by the fact that there is no way to presume the aggregate short duration cumulative probability corresponding to zero-magnitude power ramps ($\langle \phi\,(|\Delta\mu| = 0) \rangle$, that is, the “no-power-ramp” condition). The problem is circumvented by noting that $\langle \phi\,(|\Delta\mu| \leq 0) \rangle = 1$ is always true, since the per-unit magnitude of any power ramp can never exceed the turbine capacity. Thus rather than “integrating up” from $\langle \phi\,(|\Delta\mu| = 0) \rangle$, the temporal aggregate cdf is best obtained by "downward integration" as

$$\langle \phi\left(|\Delta\mu|\right)\rangle = 1 - \int_{\Delta\mu}^{1} [\langle \phi\left(\Delta\mu\right) + \phi\left(-\Delta\mu\right)\rangle].d\Delta\mu \tag{16}$$

The additional steps leading to the statistical estimate of temporal aggregate short duration power ramp cdf $\phi\left(|\Delta\mu|\right)$ are therefore as follows:

#8 The temporal aggregate pdf for unsigned short duration power ramps may be obtained as sum of the two aggregate pdf's for signed power ramps as $[\phi\left(\Delta\mu\right) + \phi\left(-\Delta\mu\right)]$.

#9 The temporal aggregate cdf for unsigned short duration power ramps may be obtained by (16). Alternatively, any suitable numerical integration method may be employed for the purpose, subject to acceptable accuracy.

3 Application background: a PAC turbine in turbulent source wind

Usefulness of the concepts presented in Sect. 2 have been listed as objective advantages "a-f" in Sect. 1. Collectively, advantages "a", "c", and "e" are indicative of limited dependence of statistical estimates on empirical data, with considerable involvement of programmable functions.

More precisely, steps #1–9 of Sect. 2.4 open a simple algorithmic route for prior evaluation of aggregate short duration power ramp distributions, which may be conveniently implemented on spreadsheets. With ideal output power curve for a commercial turbine available from the respective manufacturer, and source wind variability obtained from meteorological site measurements or estimates, the algorithmic approach fans out to several associated possibilities.

For example, comparisons can be conveniently made between expected short duration ramp distributions when different commercial makes of PAC turbine are under consideration for a specific installation site. Further, with reference to specific makes of PAC turbines for installation, comparative short duration ramp distribution studies between different sites are possible. Finally, sensitivity studies may be undertaken to follow either or both of the above, since progressive installation of PAC turbines leads to changes in short duration mean as well as standard deviation of the source wind speed. The algorithm covered by steps #1–9 is therefore robust to uncertainties of source wind statistics.

As an illustrative application of the algorithm, the widely used Vestas V-90 3 MW PAC turbine is considered for operation in turbulent conditions described by the 2005 edition of IEC 61400-1 standards [24,29]. Accordingly, Sect. 4 discusses ramp distributions for a range of short duration variability conditions. It then proceeds through the steps #7–9 stated above, evolving the temporal aggregate short duration power ramp pdf and subsequently the cdf; the temporal fraction of occurrence being determined by Rayleigh statistics. Section 5 presents a simple study to demonstrate dependence of short duration ramp distributions on the most probable short duration mean wind speed.

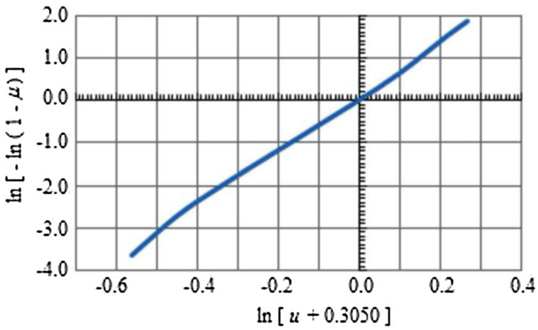

Fig. 1 Logarithmic plot (10) of the ideal zero-turbulence output coefficient for Vestas V-90 3 MW turbine between cut-in and rated values of source wind speed. Data for the plot has been obtained from [31]

Spreadsheets to support application Sects. 4 and 5 are provided as supplementary electronic material with the paper.

Preliminary calculations for the application are presented in remaining part of the present section.

3.1 The ideal zero-turbulence turbine characteristic

The Vestas V-90 3 MW enjoys considerable popularity among power utilities due to its established structural strength, robust real time performance, and time tested controls. The turbine is designed for cut-in, rated, and cut-out steady wind speeds of 3.5, 15, and 25 m/s, respectively [30]. For the three-blade nacelle configuration of 90 m swept-area diameter and 65–80 m hub-height, precise PAC output curves with streamlined source wind (at different acoustic decibels and air density) are reported in [31]. The PAC output curve specified for typical conditions of 109.4 dB(A), 1.225 kg/m^3 air density, is chosen for the present illustrative application.

Figure 1 shows a plot of $\ln[-\ln[1-\mu(u)]]$ against $\ln[u - b/a]$ between cut-in and rated values of wind speed u, with *b*/*a* in (10) set to -0.305. This value of b/a is found to bring about acceptable linear-fit between the two sets of data. The parameters a and m for the Vestas V-90 3MW are accordingly obtained as unity and 6.5274, respectively; so that $b = -0.305$. With the numerical values in place, (9) assumes a form (all quantities in pu),

$$\mu(u) = \begin{Bmatrix} 1 - \exp[-(u + 0.305)^{6.5274}]; & \text{if } 0 < u \leq 1.667 \\ 0; & \text{if } u > 1.667 \end{Bmatrix} \tag{17}$$

Following (17), the differential coefficient (12) of power ramp with respect to wind speed ramp (both in per-unit) is obtained as

$$\frac{\partial \Delta\mu}{\partial \Delta u} = 6.5274 \times \left(\left\{\hat{u} + \Delta u\right\} + 0.305\right)^{5.5274} \times \exp\left[-\left(\left\{\hat{u} + \Delta u\right\} + 0.305\right)^{6.5274}\right] \tag{18}$$

3.2 Short duration source wind statistics

In practice, the relation between short duration standard deviation σ and short duration mean wind speed $\bar{u}$ is generally site specific. Several geographic, meteorological, and engineering factors are known to contribute to the interdependence between the two [8].

For engineering convenience, the International Electrotechnical Commission periodically reports linear interdependence functions between $(\bar{u}, \sigma)$ as part of the well known IEC 61400-1 standards, which apply to potential turbine installation sites [23,24]. The functions are defined on wind speed sampled at time step of 3.0s, so that short duration variations are almost entirely accommodated.

For the present application, the interdependence function is assumed to follow the 2005 edition of the standards [24], and is given by

$$\sigma = \tau_{15}.\,(0.75\bar{u} + 5.6) \tag{19}$$

where the standard deviation is predicted by 90% quantile of wind speed at turbine hub height for ten-minute averages of mean wind speed. τ_{15} is the turbulence intensity (refer to the discussion following (2) [6]) measured at 15m sensor height. Suggested values are 0.16 for "high turbulence" (category ***A*** site conditions), 0.14 for "medium turbulence" (category ***B*** site conditions), and 0.12 for "low turbulence" (category ***C*** site conditions).

3.3 Temporal fractions of occurrence

As discussed with reference to (14–15), short duration mean wind speed at a site may have a mixed variation across long duration, which may be in parts deterministic or random. It follows that the number N in (14) and values of temporal fractions f_i $(i = 0, 1, \ldots, N)$ depend on wind variations across overall time horizon of interest. The source wind variations in turn are decided by geographic, climatic, and ambient conditions [8].

For the purpose of the current application, it is assumed that when considered over a long time span, the short duration mean wind speed $\bar{u}$ follows a Rayleigh distribution with probability density given by

$$\varphi\left(\bar{u}\right) = \left(\bar{u}/\rho^2\right).\exp\left[-\left(\bar{u}/\rho\right)^2/2\right] \tag{20}$$

Implicit in the Rayleigh distribution (20) is the well known assumption that $\bar{u}$ has two mutually perpendicular (and hence, independent) wind speed components, each of which is a normally distributed random number of identical standard deviation [28]. The assumption is generally valid across long time horizons, and on horizontal terrain without obstacles to air flow. This has led to the acceptance of the Rayleigh distribution as a performance base for wind turbine manufacturers, who often mention source long duration wind speed with corresponding *Rayleigh frequency of occurrence*

[32]. Expression (20) therefore represents a typical long duration distribution for short duration mean wind speed.

The parameter ρ in (20) represents the mode (most frequently occurring value of $\bar{u}$) of the Rayleigh distribution. If choice of turbine for a proposed installation site ensures that u_{rat} is identical to ρ by design, then (20) reduces to

$$\varphi(\bar{u}) = \bar{u}.\exp\left[-\bar{u}^2/2\right] \tag{21}$$

Though it is not mandatory to select turbines strictly according to $u_{rat} = \rho$; (21) does represent a baseline distribution with reference to such a choice. Therefore while the next section assumes (21) at an installation site proposed for the Vestas V-90 3 MW, sensitivity of short duration power change distributions to the choice of u_{rat} is presented in Sect. 5.

4 Application: power ramp distributions for baseline choice of turbine

For all studies presented in this paper, source wind speed for the Vestas V-90 3MW is considered across the range 0–3.0 pu in steps of 0.1 pu ($N + 1 = 31$ with $i = 0, 1, ..., 30$). With short duration mean wind speeds assumed to occur according to Rayleigh frequency of occurrence, the i-th temporal fraction of occurrence is obtained from (21) as

$$f_i = 0.1 \times \bar{u}_i.\exp\left[-\bar{u}_i^2/2\right] \tag{22}$$

As an implicit feature of the Rayleigh pdf (20), temporal fractions computed by (22) unconditionally satisfy the critical property (14).

For the turbulence categories specified by the 2005 edition of the IEC 61400-1 standards, (19) is used to compute the short duration standard deviation corresponding to each of the thirty-one values of $\bar{u}_i$. This meets the requirement of $(\bar{u}_i, \sigma_i)$ pairs as in step #1 of Sect. 2.4.

It is a simple matter to realise steps #2–6 of the algorithm on any commonplace spreadsheet software for the three turbulence categories. By programming appropriate functions for each of the N+1 values of $\bar{u}_i$, statistical estimate of the pdf's for short duration power ramps are obtained "around" the respective *mean wind speed*. The ***supplementary electronic materials*** accompanying this paper include illustrative spreadsheets for Sects. 4 and 5

Before proceeding beyond step #6, some insight into the nature of pdf's $\phi_i\,(\Delta\mu|\bar{u}_i)$ is useful. Accordingly, selected pdf's corresponding to turbulence categories ***A***, ***B***, and ***C*** are presented in Fig. 2. Individual plots in each correspond to different values of mean wind speed $\bar{u}_i$ as indicated (only plots at speed intervals of 0.2pu are included to retain clarity).

While numerical differences are to be expected between pdf plots of the three turbulence categories (Fig. 2), features common to all may be summarised as follows:

- Negative power ramps dominate in probability at 0.7 pu mean wind speed or higher; while positive power ramps do likewise at 0.6 pu $\bar{u}_i$ or lower. Around the two stated

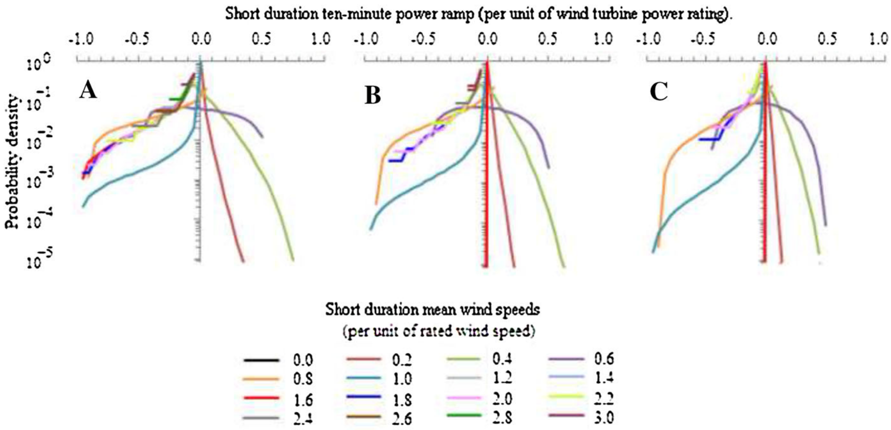

Fig. 2 Statistical estimates of selected power ramp pdf's for the Vestas V-90 3 MW, corresponding to per-unit short duration mean wind speed as indicated. **A**, **B**, and **C**, denote the IEC turbulence category assumed for source wind in each case

values, pdf's have significant spread both above and below the zero magnitude power ramp (that is, steady output power without ramping).

- At short duration mean wind speeds below 0.6 pu, probability density is found to change from about 10^{-5} to unity over a small range of positive power ramps (cut-in wind speed for the Vestas V-90 3 MW being 0.233 pu).
- At mean wind speeds above 0.7 pu, power ramp pdf's spread across the range from -1.0 pu to zero, but with a steep change close to the latter. For 1.2 pu or higher values of mean wind speed, variations occur largely within the active PAC part of (8, 9) with virtually no power change.
- Finally, for short duration mean wind speeds at 1.7 pu and beyond, rapid operation of the cut-out mechanism (the cut-out wind speed being 1.67 pu) results in domination of negative power ramps; probability density stretching from unity to 10^{-2} corresponding to ramps from zero to -1.0 pu.

Proceeding with the algorithm step #7, (22) is used to generate the Rayleigh frequency of occurrence (which for the specific example, serve as the temporal fractions of occurrence f_i) corresponding to each value of $\bar{u}_i$. Figure 3 displays the temporal aggregate short duration power ramp pdf $\langle \phi (\Delta \mu) \rangle$ (for signed power ramps $\Delta \mu$) as obtained by (15). For all three turbulence categories, "near unity" aggregate probability density is noted for zero magnitude ramps. The temporal aggregate pdf drops to 10^{-3} or less for "rated negative ramps" ($\Delta\ \mu\ \lambda\ -1.0$ pu) as decided by turbulence category; with similar drop at "half-of-rated positive ramps" ($\Delta\ \mu\ \lambda\ +0.5$ pu). Expectedly for higher turbulence categories, likelihood of large power ramps becomes significant.

Additionally included in Fig. 3 are plots from ensemble estimate of pdf for the Vestas V-90 3 MW, as reported in [33]. The ensemble estimates from [33] are found to be comparable to "worst-case" statistical estimates for IEC turbulence category ***C***, and in fact show marginally lower probability for comparable power ramp magnitudes. Possible contributors to the improvement in probability are:

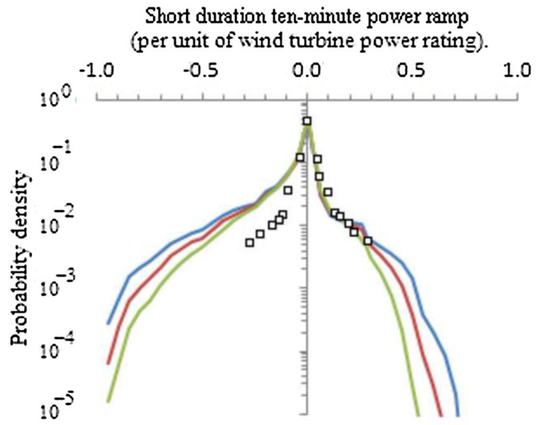

Fig. 3 Temporal aggregate power ramp pdf's obtained by aggregation of $\phi_i\ (\Delta\mu|\bar{u}_i)$ for the Vestas V-90 3 MW; assuming temporal fractions of occurrence according to (22). Turbulence categories are **A** (blue), **B** (red), and **C** (green) as per IEC 61400-1 standards. The square symbols indicate ensemble estimates (based on practical field data) for the Vestas V-90 3 MW, as reported in [33]

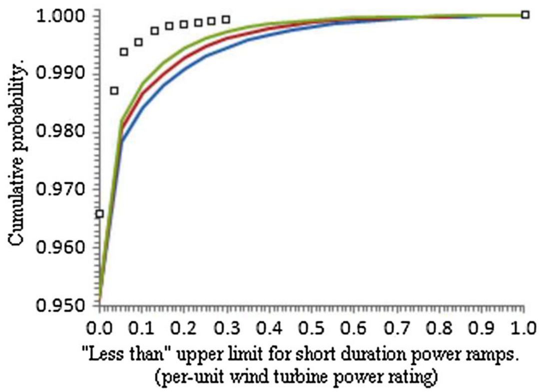

Fig. 4 Statistical estimate of cdf's corresponding to the temporal aggregate power ramp pdf's shown in Fig. 3 for the Vestas V-90 3 MW. Turbulence categories are **A** (blue), **B** (red), and **C** (green) as per IEC standards. Values obtained by numerical integration across practical field recordings (as reported in [33], and presented in Fig. 3) are shown by square symbols

- Relatively infrequent operation of the turbine around cut-out, which is reflected by symmetry of ensemble estimates about the vertical axis in Fig. 3. Temporal fractions of occurrence for the practical field data presented in [33] are possibly different from the Rayleigh frequency (22).
- Practical measurements on the Vestas V-90 3 MW include filtering effect of turbine dynamics on short duration power variations, with consequent reduction of probability at most power ramps.

Implication of the aforementioned spread of pdf's is better interpreted from the "worst-case" temporal aggregate short duration power ramp cdf's, computed according to algorithm steps #8–9 of Sect. 2.4, and presented for all three IEC turbulence categories in Fig. 4. Further, data from the pdf reported in [33] is numerically integrated by trapezoidal method (similar to steps #8–9, Sect. 2.4), and included in the same figure as an ensemble estimate of cdf.

The "worst-case" nature of statistical estimates (algorithm steps #1–9, Sect. 2.4) is immediately evident from Fig. 4, as the typical ensemble estimate cdf for the Vestas V-90 3 MW [33] accommodates short duration power ramps up to 0.06 pu within 99% cumulative probability; while statistical estimate for IEC turbulence category ***C*** would

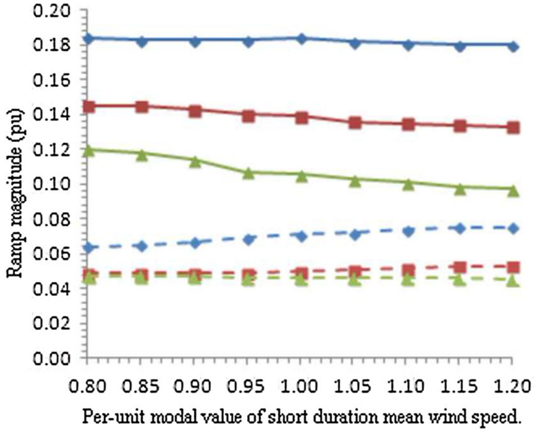

Fig. 5 Maximum ramp magnitudes for the Vestas V-90 3 MW operating in source wind as per IEC 61400-1 standards; obtained as statistical estimates corresponding to cumulative probability of 99% (continuous) and 98% (broken line). Turbulence categories are **A** (blue), **B** (red), and **C** (green)

make one expect ramps up to about 0.12 pu. For turbulence of IEC category $\boldsymbol{A}$, power ramps covered within 99% probability would be $|\Delta\mu| \leq 0.182$ pu.

In the next section, the above studies are extended to analyse sensitivity of temporal aggregate short duration power ramp cdf′s to temporal fractions of occurrence $\{f_i\}$, again for the Vestas V-90 3 MW in turbulent source wind according to the IEC 61400-1 standards.

5 Application: aggregate power ramp distributions for different temporal fractions of occurrence

In practice short duration power ramp distributions, when aggregated over different time horizons for a specific make of turbine, may differ according to local source wind conditions as well as seasonal variations. Within a turbine cluster, proximity effects between individual units (such as wakes and tower shadows) may introduce further differences between their power ramp distributions; statistics for the entire footprint being a spatial aggregation across all units.

The application of Sect. 4 is now extended to show that statistical estimates can serve as a quick and convenient route to study sensitivity of short duration power ramp distributions to temporal fractions of occurrence.

In Sect. 4, the Vestas V-90 3 MW was considered for a prospective installation site at which a short duration mean wind speed of 1.0 pu (15 m/s as specified for the turbine [31]) was assumed to be the most frequent ($\rho = 1.0$ in (20) with f_i according to (22)). In the present section, it is assumed that the most probable short duration mean wind speed at the site may vary between 0.8 and 1.2 pu subject to source wind conditions, seasonal variations, and proximity effects.

"Less than" upper limits that cover power ramps ($|\Delta\mu|$) within high cumulative probability of 99 and 98% are presented in Fig. 5 for all three IEC turbulence categories. The trends observed are decided by mutually conflicting influence of two factors:

- Progressively high standard deviation with increasing short duration mean wind speed according to (19), and
- Output fraction $\mu(\bar{u})$ by (8, 9) moving deeper into the active PAC range of wind speed (within which output power is steady with $\mu(\bar{u}) = 1$).

For a cumulative probability of 99% of short duration power ramps, the Vestas V90 3 MW may at its worst expect 0.12 pu power ramps with source wind of IEC category ***C***; while corresponding ramp limits for turbulence category ***A*** and ***B*** are 0.184 and 0.145 pu respectively. For either turbulence category, ramping within 99% probability improves as the turbine moves deeper into PAC operation; the improvement being particularly significant for category ***C*** source wind, with maximum ramp magnitude dropping to 0.097 pu at 1.2 pu mean wind speed. Of the two factors mentioned above, the turbine is strongly influenced by the former when performing in turbulence of categories ***A*** or ***B***; while for IEC category ***C***, the latter factor dominates.

Virtually a reversal between influences of the two factors is observed within the one percent difference of cumulative probability. Not only do maximum ramp limits drop by a factor of half or less between cumulative probability of 99 and 98%, but the trends are found to reverse as well. For performance in turbulent wind of IEC category ***A***, change of "less than" ramp limit from 0.064 pu upward is noted, as mean wind speed changes from 0.8 to 1.2pu. Corresponding trend for turbulence category ***B*** is 0.049pu upward. A minor drop of ramp limit, from 0.047pu to 0.045pu, is observed in case of turbulence category ***C***.

6 Conclusions

The easy-to-use algorithmic approach introduced in this paper allows statistical estimate of short duration power ramp distributions (both pdf's and cdf's) without elaborate compilation of field data ensembles. The modest data requirements include basic short duration statistical properties of the source wind. For sites that meet IEC 61400-1 standards, such source wind statistics are well reported; a feature that adds to usefulness and compatibility of statistical estimates.

Illustrative applications of the proposed algorithmic procedure have been presented for the Vestas V-90 3 MW turbine. The presentation is indicative of possible rapid evaluation of worst case output power ramp statistics for available makes of turbines. For any existing or proposed installation site, comparative study between candidate turbines (including sensitivity analysis) may thus be undertaken without heavy computational burden or elaborate field data requirements.

Further if changes in short duration mean wind speed and standard deviation with progressive installation of turbines are tracked to acceptable accuracy, then the algorithm can be extended to turbine clusters. Evolution of such extensions can be appropriate subject for future research.

References

1. Langreder, W., Kaiser, K., Hohlen, H., Hojstrup, J.: Turbulence correction for power curves. In: Presented at the Euro. Wind energy conf. & Exh, London (2004)

2. GE energy: western wind and solar integration study. Natl. Ren. Energy Lab., Golden. http://www.nrel.gov/docs/fy10osti/47434.pdf (2010). Accessed 25 Jun 2017
3. EnerNex Corp: eastern wind integration and transmission study. Natl. Ren. Energy Lab., Golden. http://www.nrel.gov/docs/fy11osti/47078.pdf (2011). Accessed 25 Jun 2017
4. Hittinger, E., Apt, J., Whitacre, J.F.: The effect of variability-mitigating market rules on the operation of wind power plants. Energy Syst. **5**, 737–766 (2014)
5. Wu, A., Philpott, A., Zakeri, G.: Investment and generation optimization in electricity systems with intermittent supply. Energy Syst. **8**, 127–147 (2017)
6. Manwell, J.F., McGowan, J.G., Rogers, A.L.: Wind Energy Explained: Theory, Design, and Application. Wiley, Chichester (2009)
7. Rinne, H.: The Weibull Distribution: A Handbook. Chapman & Hall/CRC, Boka Raton (2009)
8. Frandsen, S.T.: Turbulence and turbulence generated structural loading in wind turbine clusters. Risø Natl. Lab., Roskilde. http://orbit.dtu.dk/fedora/objects/orbit:79899/datastreams/file_269c3f19-0001-4e41-b754-b5b322a826cb/content (2007). Accessed 25 Jun 2017
9. Lee D., Baldick R.: Limiting ramp rate of wind power output using a battery based on the variance gamma process. In: Presented at the intl. conf. ren. energies & power qual., Santiago de Compostela, 2012. http://www.icrepq.com/icrepq' 12/771-lee.pdf (2012). Accessed 25 Jun 2017
10. Fox, B., Flynn, D., Bryans, L., Jenkins, N., Milborrow, D., O'Malley, M., Watson, R., Anaya-Lara, O.: Wind Power Integration: Connection and System Operational Aspects. IET, London (2007)
11. USDOE-EERE: dispatchability. http://energy.gov/eere/sunshot/dispatchability (2015). Accessed 25 Jun 2017
12. IEA wind task 5: design and operation of power systems with large amounts of wind power: state-of-the-art report. VTT-St. Tech. Res. Center, Espoo. http://www.ieawind.org/annex_XXV/Publications/W82.pdf (2007). Accessed 25 Jun 2017
13. Wan, Y-h.: Analysis of wind power ramping behavior in ERCOT. Natl. Ren. Energy Labs., Golden. http://www.nrel.gov/docs/fy11osti/49218.pdf (2011). Accessed 25 Jun 2017
14. Gevorgian, V., Corbus, D.: Ramping performance analysis of the Kahuku wind-energy battery storage system. Natl. Ren. Energy Lab., Golden. http://www.nrel.gov/docs/fy14osti/59003.pdf (2013). Accessed 25 Jun 2017
15. Foster, R.: Windpower Engineering & Development: the Technical Resource for Wind Profitability. WTWH Media LLC., Cleveland. https://www.neces.com/assets/WindPower-Engineering-A123-Systems_Reprint1.pdf (2013).Accessed 25 Jun 2017
16. Kirby, B.J.: Frequency regulation basics and trends. OR Natl. Lab., Oak Ridge. http://www.consultkirby.com/files/TM2004-291_Frequency_Regulation_Basics_and_Trends.pdf (2004). Accessed 25 Jun 2017
17. Bartels, M., Gatzen, C., Peek, M., Schulz, W., Wissen, R., Jansen, A., Molly, J.P., Neddermann, B., Gerch, H.-P., Grebe, E., Saßnick, Y., Winter, W.: Planning of the grid integration of wind energy in Germany onshore and offshore up to the year 2020. Deutsche Energie-Agentur GmbH, Berlin. https://docs.wind-watch.org/dena-integratingwind2020.pdf (2005). Accessed 25 Jun 2017
18. Hodge, B.M., Shedd, S., Florita, A.: Examining the variability of wind power output in the regulation time frame. In: Presented at the Intl. Wshop. Large-scale integ. of wind power into power systems & trans. nets. for offshore wind power plants, Lisbon. http://www.ourenergypolicy.org/wp-content/uploads/2012/08/55967.pdf (2012). Accessed 25 Jun 2017
19. Vestas Wind Systems A/S: products: options and solutions. https://www.vestas.com/en/products/options_and_solutions#!plant-optimisation (2017). Accessed 25 Jun 2017
20. Suzlon Group: Suzlon products. http://www.suzlon.com/products (2017). Accessed 25 Jun 2017
21. Das, A.K.: An empirical model of power curve of a wind turbine. Energy Syst. **5**, 507–518 (2014)
22. Wan Y-h., Ela E., Orwig K.: Development of an equivalent wind plant power curve. In: Presented at the windPower 2010 conf., Dallas (2010)
23. IEC: wind turbine generator systems (Part-1: safety requirements). IEC. Intl. Std. 61400-1:1999 (1999)
24. IEC: wind turbines (part-1: design requirements). IEC. Intl. Std. 61400-1:2005 (2005)
25. Justus, C.G.: Winds and Wind System Performance. Franklin Institute Press, Philadelphia (1978)
26. Yin, X., Goudriaan, J., Latinga, E.A., Vos, J., Spiertz, H.J.: A flexible sigmoid function of determinate growth. Ann. Bot. **91**, 361–371 (2003)
27. Weibull, W.: A statistical distribution function of wide applicability. J. Appl. Mechs. **18**, 293–297 (1951)

28. Tuller, S.E., Brett, A.C.: The characteristics of wind velocity that favor the fitting of a Weibull distribution in wind speed analysis. J. Clim. Appl. Meteorol. **23**, 124–134 (1984)
29. Imamura H., Kogaki T., Tanagaki S., Matsumiyua H.: Evaluation of turbulence model in IEC 61400-1 Ed.3 by NEDO guideline measurement data. Proc. Jpn. Wind Energy Symp. **31**, 157-160 (2009). https://www.jstage.jst.go.jp/article/jweasympo/31/0/31_157/_pdf. Accessed 25 Jun 2017
30. Vestas: procurement V90-3MW. http://www.vestas.com/en/wind-power-plants/procurement/turbine-overview/v90-3.0-mw.aspx#/vestas-univers (2011). Accessed 25 Jun 2017
31. Vestas R&D: General specification for V90–3.0 MW, 60 Hz variable speed turbine. Ringkøbing: vestas wind systems A/S. http://www.gov.pe.ca/photos/sites/envengfor/file/950010R1_V90-GeneralSpecification.pdf. Accessed 25 Jun 2017
32. Rivkin, D.A., Liddell, A., Silk, L.: Wind Turbine Systems: The Art and Science of Wind Power, pp. 76–77. Jones & Bartlett Pubs, Burlington (2013)
33. van Dam C.P., de Mello P., Shiu H., Kamisky R.: Overview of wind forecasting research efforts at UC Davis. In: Presented at the CEC Wshp. Solar & Wind Frcstg: achieving a 33% Soln., Sacramento. http://www.energy.ca.gov/research/notices/2011-12-16_workshop/presentations/08_UCDavis-Van_Dam.pdf (2011). Accessed 25 Jun 2017